第 32 卷第 8 期 无 机 化 学 学 报 Vol.32 No.8
2016 年 8 月 CHINESE JOURNAL OF INORGANIC CHEMISTRY 1487-1494

4,4′-联吡啶桥联的三个铜有机膦酸配合物的合成、结构及磁性

叶文鹏 陈 铭 杨 意 查丽琴 马运声* 袁荣鑫*
(常熟理工学院化学与材料工程学院,江苏省新型功能材料重点建设实验室,常熟 215500)

摘要: 在水热条件下,以 *N*-氧化-2-吡啶膦酸(H_2L)为主配体,4,4′-联吡啶(bpy)为桥联配体,合成了 3 个铜有机膦酸配合物:$\{[Cu(L)(bpy)_{0.5}(H_2O)]\cdot 2H_2O\}_n$(**1**), $\{[Cu(HL)_2(bpy)]\cdot 4H_2O\}_n$(**2**)和$\{[Cu_2(L)_2(bpy)]\cdot 3H_2O\}_n$(**3**)。配合物 **1** 中,相邻的铜离子由 2 个膦酸根连成二聚体,二聚体之间通过 bpy 桥联成一维链。配合物 **2** 中,单核$[Cu(HL)_2]$被 bpy 连接成一维链。配合物 **3** 中,四聚体$[Cu_2(L)_2]_2$ 被 bpy 连接成“砖块状”结构的二维层。磁性研究表明,配合物 **1** 和 **3** 中铜离子之间存在反铁磁性耦合。

关键词: 铜配合物; 有机膦酸; 4,4′-联吡啶; 磁性
中图分类号: O614.121 **文献标识码**: A **文章编号**: 1001-4861(2016)08-1487-08
DOI: 10.11862/CJIC.2016.196

Syntheses, Structures and Magnetic Properties of Three Copper Phosphonates Bearing 4,4′-Bipyridine Bridge

YE Wen-Peng CHEN Ming YANG Yi ZHA Li-Qin MA Yun-Sheng* YUAN Rong-Xin*
(*Key Laboratory of Advanced Functional Materials, School of Chemistry and Materials Engineering, Changshu Institute of Technology, Changshu, Jiangsu* 215500, *China*)

Abstract: Three copper phosphonates $\{[Cu(L)(bpy)_{0.5}(H_2O)]\cdot 2H_2O\}_n$ (**1**), $\{[Cu(HL)_2(bpy)]\cdot 4H_2O\}_n$ (**2**) and $\{[Cu_2(L)_2(bpy)]\cdot 3H_2O\}_n$ (**3**) (H_2L=2-pyridyl-*N*-oxide phosphonic acid, bpy=4,4′-bipyridine) were synthesized under hydrothermal conditions. In compound **1**, the adjacent Cu(Ⅱ) ions are connected by two phosphonate ligands into a dimer, which are bridged by bpy into 1D chain. Compound **2** has a 1D chain structure with $[Cu(HL)_2]$ as junction and bpy as linker. Compound **3** has a brick-like 2D structure with $[Cu_2(L)_2]_2$ as junction and bpy as spacer. The magnetic property studies of compounds **1** and **3** reveal that antiferromagnetic interactions are mediated between the copper ions. CCDC: 1477698, **1**; 1477699, **2**; 1477700, **3**.

Keywords: copper complex; phosphonic acid; 4,4′-bipyridine; magnetic property

0 Introduction

Metal phosphonates have received great attention for their versatile structures and potential applications in the fields of magnetism, proton conductivity, catalysis and gas adsorption[1]. The monophosphonic acid R-PO_3H_2 (R =aryl, alkyl) prefer to form layered or polynuclear structures with transition metal ions[2]. By introducing a functional group such as hydroxyl[3], amino[4], carboxylate[5], crown-ether[6], a second phosphonate group[7], compounds with new structure and properties can be obtained. In addition, introducing a co-ligand in the reaction system, such as 1,4-bis(imidazol-1-ylmethyl)benzene[8], 6-chloro-2-hydroxypyridine (Hchp)[9] or di-2-pyridyl ketone (dpk)[10], would help the formation of the new types of structure.

收稿日期:2016-05-07。收修改稿日期:2016-06-28。
江苏省高校自然科学重大项目(No.14KJA150001)和江苏省六大人才高峰计划资助。
*通信联系人。E-mail:myschem@cslg.edu.cn,yuanrx@cslg.edu.cn;会员登记号:S06N6527M1303。

In the previous work, we have shown that one-dimensional copper phosphonates $[Cu_2X_2(C_5H_4NOPO_3)_2][Cu(H_2O)_6]\cdot 2H_2O$ [X=Cl, Br] and $CuX(C_5H_4NOPO_3H)\cdot H_2O$ (X=Cl, Br) based on 2-pyridyl-N-oxide phosphonic acid (H_2L) can be obtained under solution method with halides as bridge[11]. To explore new types of copper (2-pyridyl-*N*-oxide)phosphonate compounds, we are to incorporate a longer bridge (4,4′-bipyridine, bpy) in the reaction system. Fortunately, three types of copper phosphonates with 1D and 2D structures are resulted in. Herein we report the syntheses, characterization and magnetic properties of $\{[CuL(bpy)_{0.5}(H_2O)]\cdot 2H_2O\}_n$ (**1**), $\{[Cu(HL)_2(bpy)]\cdot 4H_2O\}_n$ (**2**) and $\{[Cu_2(L)_2(bpy)]\cdot 3H_2O\}_n$ (**3**).

1 Experimental

1.1 Materials and methods

H_2L was prepared according to the literature method[12]. All other starting materials were purchased as reagent grade and used without further purification. Elemental analyses were performed on a Perkin Elmer 240C elemental analyzer. The IR spectra were obtained as KBr disks on a VECTOR 22 spectrometer. Powder X-ray diffraction patterns (PXRD) were determined with Rigaku-D/Max-2200 X-ray diffractometer with Cu $K\alpha$ radiation (λ=0.154 18 nm). The magnetic susceptibility data were obtained on a microcrystalline sample, using a Quantum Design MPMS-XL7 SQUID magnetometer. Diamagnetic corrections were made for both the sample holder and the compounds estimated from Pascals constants[13].

1.2 Syntheses

$\{[Cu(L)(bpy)_{0.5}(H_2O)]\cdot 2H_2O\}_n$ (**1**): H_2L (0.017 5 g, 0.10 mmol), $Cu_2(OH)_2CO_3$ (0.007 3 g, 0.033 mmol), bpy (0.015 6 g, 0.10 mmol) and 2 mL H_2O were put into a 6 mL glass tube, which was sealed and heated at 120 ℃ for 2 days. After slow cooling to room temperature, pale green block crystals were obtained. Yield: 63% based on $Cu_2(OH)_2CO_3$. Anal. Calcd. for $C_{10}H_{14}CuN_2O_7P$(%): C, 32.57; H, 3.83; N, 7.60. Found (%): C, 32.25; H, 3.66; N, 7.36. IR (KBr, cm^{-1}): 3 372 (s), 3 109(s), 1 606 (s), 1 407(s), 1 265 (m), 1 201(vs), 1 082(s), 967 (s), 837(s), 557 (s), 503(s).

$\{[Cu(HL)_2(bpy)]\cdot 4H_2O\}_n$ (**2**): The synthesis of **2** is similar to **1** except changing the molar ratio of starting materials to 2∶1∶1. Yield: 33% based on $Cu_2(OH)_2CO_3$. Anal. Calcd. for $C_{20}H_{26}CuN_4O_{12}P_2$ (%): C, 37.54; H, 4.10; N, 8.76. Found (%): C, 37.21; H, 3.82; N, 8.48. IR (KBr, cm^{-1}): 3415 (vs), 3 123 (vs), 1 620 (m), 1 405 (vs), 1 222(s), 1 176(s), 1 070 (s), 923 (m), 773(m).

$\{[Cu_2(L)_2(bpy)]\cdot 3H_2O\}_n$ (**3**): The synthesis of **3** is similar to **1** except $Cu(OH)_2$ was chosen as the copper source. Yield: 48% based on $Cu(OH)_2$. Anal. Calcd. for $C_{20}H_{24}Cu_2N_4O_{12}P_2$ (%): C, 34.24; H, 3.45; N, 7.99. Found(%): C, 34.01; H, 3.66; N, 8.25. IR (KBr, cm^{-1}): 3 370 (vs), 3 124 (vs), 1 611 (m), 1 405(vs), 1 177 (vs), 1 106 (vs), 984 (s), 833 (m), 543(m).

1.3 X-ray crystallographic analyses

Single crystal data were collected on a Rigaku SCX mini CCD diffractometer by using graphite-monochromated Mo $K\alpha$ radiation (λ=0.071 073 nm) at room temperature. Cell parameters were refined by using the program CrystalClear [14] on all observed reflections. The collected data were reduced by using the program CrystalClear, and an absorption correction (multi-scan) was applied. The reflection data were also corrected for Lorentz and polarization effects. The structures were solved by direct methods and refined on F^2 by full matrix least squares using SHELXTL[15]. All the non-hydrogen atoms were located from the Fourier maps, and were refined anisotropically. All H atoms were refined isotropically, with the isotropic vibration parameters related to the non-H atom to which they are bonded. Crystallographic and refinement details of **1**~**3** are listed in Table 1. Selected bond lengths and angles are given in Table 2 for **1**, **2** and **3**, respectively.

CCDC: 1477698, **1**; 1477699, **2**; 1477700, **3**.

Table 1 Crystal data and structure refinements for 1, 2 and 3

	1	2	3
Formula	$C_{10}H_{14}CuN_2O_7P$	$C_{20}H_{26}CuN_4O_{12}P_2$	$C_{20}H_{24}Cu_2N_4O_{12}P_2$
Formula weight	368.74	639.93	701.45

Continued Table 1

Crystal system	Triclinic	Monoclinic	Monoclinic
Space group	$P\bar{1}$	$P2_1/n$	$P2_1/c$
a / nm	0.816 62(16)	0.807 00(16)	0.822 10(16)
b / nm	0.949 50(19)	1.431 8(3)	2.088 2(4)
c / nm	1.009 2(2)	1.104 8(2)	1.516 1(3)
α / (°)	69.64(3)	90	90
β / (°)	71.00(3)	90.68(3)	97.94(3)
γ / (°)	89.72(3)	90	90
V	688.5(3)	1 276.5(4)	2 577.8(9)
Z	2	2	4
D_c / (g·cm^{-3})	1.779	1.665	1.807
μ / mm^{-1}	1.737	1.052	1.846
F(000)	376	658	1424
R_{int}	0.055 9	0.045 6	0.039 9
GOF on F^2	1.101	1.044	1.075
R_1, wR_2 [$I>2\sigma(I)$]	0.057 3, 0.089 2	0.035 7, 0.082 1	0.030 1, 0.077 9
R_1, wR_2 (all data)	0.083 9, 0.094 7	0.046 1, 0.085 5	0.032 0, 0.079 2
$(\Delta\rho)_{max}$, $(\Delta\rho)_{min}$ / (e·nm^{-3})	383, −443	326, −343	416, −572

Table 2　Selected bond lengths (nm) and angles (°) for compounds 1, 2 and 3

			1		
Cu1-O1	0.193 9(3)	Cu1-O1W	0.234 3(4)	Cu1-O4	0.198 3(4)
Cu1-N2	0.202 5(4)	Cu1-O3A	0.195 0(3)		
O1-Cu1-O1W	106.10(13)	O1-Cu1-O4	92.68(15)	O1-Cu1-N2	92.47(15)
O1-Cu1-O3A	159.72(13)	O1W-Cu1-O4	89.32(15)	O1W-Cu1-N2	90.57(15)
O1W-Cu1-O3A	93.64(13)	O4-Cu1-N2	174.68(16)	O3A-Cu1-O4	82.77(15)
O3A-Cu1-N2	91.93(15)				
			2		
Cu1-O2	0.196 6(2)	Cu1-O4	0.243 0(2)	Cu1-N2	0.200 9(2)
O2-Cu1-O4	85.38(7)	O2-Cu1-N2	89.74(8)	O4-Cu1-N2	90.05(9)
			3		
Cu1-O2	0.194 6(2)	Cu1-N3	0.200 7(2)	Cu1-O6	0.193 7(2)
Cu1-O8	0.199 5(2)	Cu2-O1	0.191 5(2)	Cu2-O4	0.204 1(2)
Cu2-O6	0.234 9(2)	Cu2-N4B	0.202 1(2)	Cu2-O7A	0.194 7(2)
O2-Cu1-O8	174.70(8)	O2-Cu1-O6	91.10(8)	O2-Cu1-N3	90.47(8)
O2-Cu1-O12	87.07(7)	O6-Cu1-O12	101.10(8)	O6-Cu1-O8	92.30(8)
O8-Cu1-O12	88.28(9)	O6-Cu1-N3	167.51(9)	O12-Cu1-N3	91.35(9)
O8-Cu1-N3	87.09(9)	O1-Cu2-O6	89.20(7)	O1-Cu2-N4B	177.28(9)
O1-Cu2-O7A	87.40(8)	O6-Cu2-O7A	115.07(7)	O6-Cu2-N4B	88.08(8)
Cu1-O6-Cu2	100.90(8)	O7A-Cu2-N4B	93.88(8)		

Symmetry codes: A: 1−x, 1−y, 1−z for **1**; A: 2−x, 2−y, 2−z; B: 1−x, 0.5+y, 1.5−z for **3**

2 Results and discussion

2.1 Syntheses

The molar ratio of the starting materials and copper source are important for the formation of the pure product. When $Cu(OH)_2$ was used as the copper source, compounds **1**, **2** and **3** can be obtained by varying the molar ratio. While, there are some undetermined powder formed simultaneously with compounds **1** and **2**. When $Cu_2(OH)_2CO_3$ was employed as the starting material, pure compounds **1** and **2** could be formed. In addition, we found the crystal color of compound **2** will change from blue to green if keeping the crystal in the mother liquid over two days. However, the trying to determine the crystal structure was not successful. Other copper sources such as $CuSO_4$, $Cu(NO_3)_2$, $Cu(ClO_4)_2$, $CuCl_2$ have also been employed in the reaction system, however, only precipitate formed. Thus, we think the acid-base neutralization between phosphonic acid and basic copper source should be important for the crystallization of the final product.

2.2 Structure description

2.2.1 Crystal structure of compound **1**

Compound **1** crystallizes in the triclinic space group $P\bar{1}$. The asymmetric unit contains one Cu(Ⅱ) ion, one L^{2-}, 0.5 bpy, one coordinated water, and two lattice water molecules. The Cu(Ⅱ) ion locates in the tetragonal pyramidal geometry coordinated with atoms O1, O4, O3A, O1W and N2. O1W sites on the vertex with Cu1-O1W distance of 0.234 3 (4) nm, which is longer than other Cu-O bond lengths (0.193 9(3)~0.198 3(3) nm) (Fig.1). The phosphonate ligand acts as tridentate chelating and bridging ligand to coordinate with two equivalent Cu(Ⅱ) ions. The Cu1 … Cu1A distance is 0.321 5(2) nm. The binuclear units are bridged by bpy into uniform 1D chain. These chains are linked by hydrogen bonds into 3D network (Fig.2).

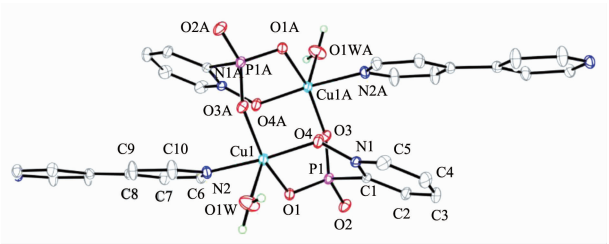

Thermal ellipsoid at 30% probability; Symmertry codes: A: 1–*x*, 1–*y*, 1–*z*

Fig.1 View of the coordination environment around the Cu(Ⅱ) ions and the coordination mode of the ligands in **1**

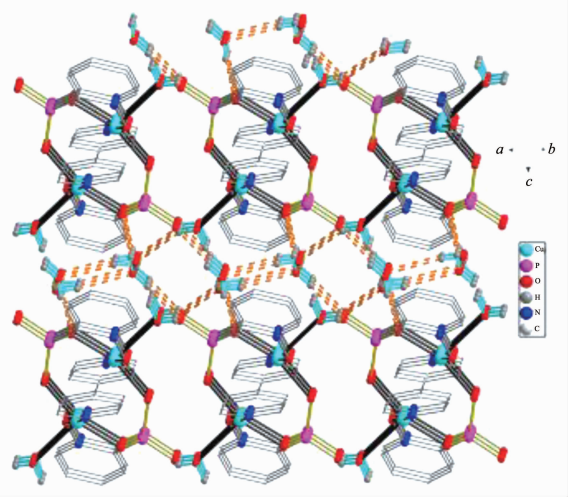

Fig.2 Hydrogen bond connected packing diagram of compound **1**

2.2.2　Crystal structure of compound **2**

Compound **2** crystallizes in the monoclinic space group $P2_1/n$. The asymmetric unit contains 0.5 Cu(Ⅱ) ion, one HL^-, 0.5 bpy and four lattice water molecules. The Cu1 atom locates at an inversion center and has an octahedral geometry with six positions occupied by O2, O4, N2, O2A, O4A and N2A from two HL^- and two bpy ligands. The bond length of Cu1-O2 is 0.196 6(2) nm, shorter than Cu1-O4 bond length (0.243 0(2) nm) (Fig.3). The phosphonate ligand provides O2 and N-oxide oxygen (O4) atoms to chelate with Cu1 atom forming a six member ring. One oxygen atom (O1) of the phosphonate is protonated with the P1-O1 bond length of 0.156 9(2) nm. Adjacent Cu(Ⅱ) ions are bridged by bpy into 1D chain with Cu1…Cu1B distance of 1.104 8(2) nm. The chains are connected by hydrogen bonds into a three dimensional network (Fig.4).

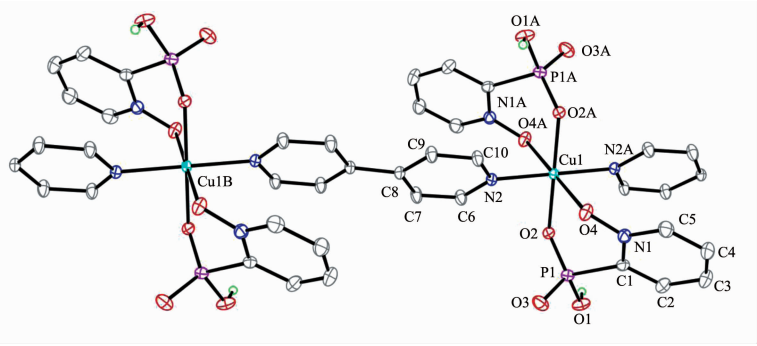

Thermal ellipsoid at 30% probability; Symmertry codes: A: $-x$, $2-y$, $1-z$; B: $-x$, $2-y$, $2-z$

Fig.3　View of the coordination environment around the Cu(Ⅱ) ion and the coordination mode of the ligands in **2**

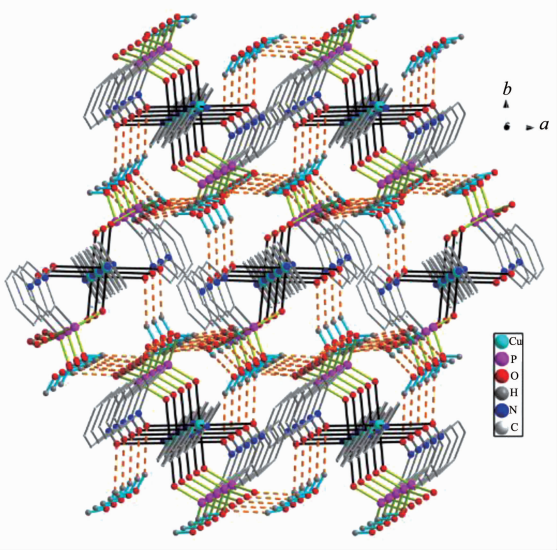

Fig.4　Hydrogen bond connected packing diagram of compound **2**

2.2.3　Crystal structure of compound **3**

Compound **3** crystallizes in the monoclinic space group $P2_1/n$. The asymmetric unit contains two independent Cu(Ⅱ) ions, two L^{2-}, one bpy and three lattice water molecules. The Cu1 atom has a planar coordination environment with four positions occupied by O2, O6 and O8 from two L^{2-} ligands and N3 from one bpy (Fig.5). The Cu1-O bond lengths fall in the normal range[16]. The Cu2 atom has a square pyramidal geometry. Four basal positions are filled with O1, O4 and O7A from two L^{2-} ligands and N4B from one bpy. The axial position is filled with O6 from the third L^{2-}

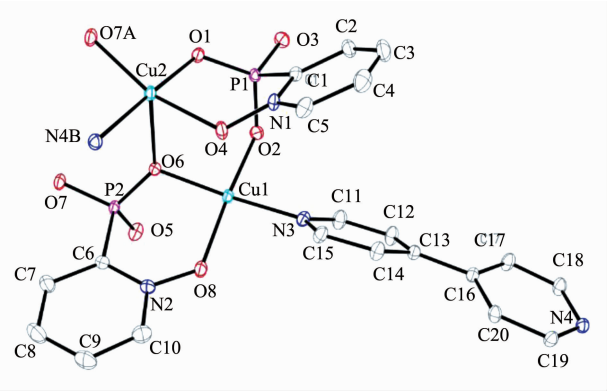

Thermal ellipsoid at 30% probability; Symmetry codes: A: 2–*x*, 2–*y*, 2–*z*; B: 1–*x*, 0.5+*y*, 1.5–*z*

Fig.5 View of the coordination environment around the Cu(Ⅱ) ions and the coordination mode of the ligands in **3**

ligand. Cu1 and Cu2 atoms are bridged by two phosphonate ligands into a dimer. The dimers are further linked by two O-P-O groups into a tetramer $[Cu_2(L)_2]_2$. Adjacent tetramers are bridged by bpy ligands into a brick-like 2D layer (Fig.6).

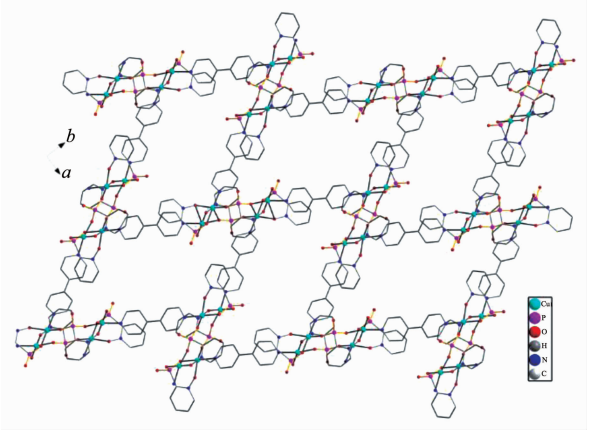

Fig. 6 2D structure of compound **3**

2.3 Powder X-ray diffraction measurements

Phase purities of the bulky materials of **1~3** were confirmed by powder X-ray diffraction (PXRD) patterns (Fig.7). The experimental and simulated PXRD patterns agree well with each other, confirming the good phase purity.

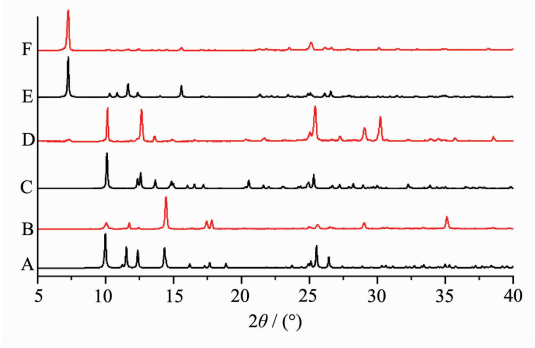

Fig.7 Simulated (A, C, E) and experimental (B, D, E) PXRD patterns for compounds **1**, **2** and **3**, respectively

2.4 Magnetic properties

The temperature-dependent molar magnetic susceptibilities of **1** and **3** were measured at 2 kOe in the temperature range of 2~300 K. The χ_M and $\chi_M T$ vs T plots for **1** are shown in Fig.8. The room temperature magnetic moment per Cu(Ⅱ) is 1.79μ_B, close to the theoretical value (1.73μ_B) for an isolated spin S =1/2. On cooling, the $\chi_M T$ value decreases gradually indicating an antiferromagnetic coupling between the Cu(Ⅱ) ions. The susceptibility data were analyzed by Bleaney-Bowers expression based on a Heisenberg Hamiltonian $H=-2JS_1S_2$[13]:

$$\chi = \frac{2Ng^2\beta^2}{kT} \times \frac{1}{3+e^{\frac{-2J}{(kT)}}} \quad (1)$$

$$\chi_M = \frac{\chi}{1-[2zj'/(Ng^2\beta^2)]\chi} \quad (2)$$

Where $2J$ is the singlet-triplet energy gap, zj' accounts for the exchanges across the bpy and N, g, β and k have their usual meanings. A good fit resulted in the solid line in Fig.8, with the parameters: g=2.05, J=−5.4 cm^{-1}, zj'=−4.5 cm^{-1}.

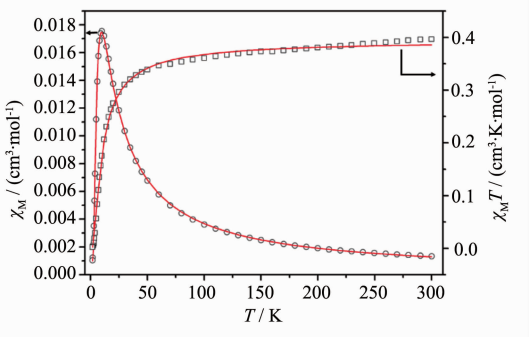

Solid line shows the best fit of the data

Fig.8　Plots of χ_M or $\chi_M T$ vs T for **1**

Fig.9 shows the χ_M and $\chi_M T$ vs T plots for **3**. The room temperature effective magnetic moment of 2.68μ_B per Cu_2 is close to the expected spin only value for S=1/2 (2.83μ_B). The continuous decreasing of $\chi_M T$ upon cooling confirms dominant antiferromagnetic interactions between the adjacent Cu(Ⅱ) ions. According to the structure of compound **3**, the magnetic exchanges between the Cu(Ⅱ) ions may be propagated through the μ-O(P) and O-P-O bridges within the $[Cu_2(L)_2]_2$ tetramer and bpy between the plane. It is well known that comparing the μ-O (P) bridge, three-atom bridge O-P-O play a negligible role in propagating the magnetic exchange. Therefore the magnetic exchange through μ-O(P) bridge is dominant. The susceptibility data were analyzed by Bleaney-Bowers expression based on a Heisenberg Hamiltonian $H=-2JS_1S_2$. A good fit resulted in the solid line in Fig.9, with the parameters: g=2.21, J=−5.8 cm^{-1}, zj'= 0.28 cm^{-1}.

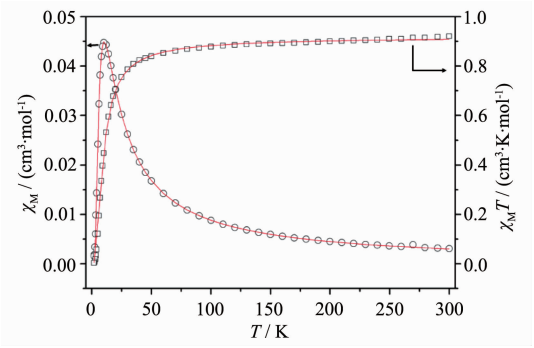

Solid line refers to the best fit of the data

Fig.9　Plots of χ_M or $\chi_M T$ vs T for **3**

3 Conclusions

Three copper phosphonates $\{[CuL(bpy)_{0.5}(H_2O)]\cdot 2H_2O\}_n$ (**1**), $\{[Cu(HL)_2(bpy)]\cdot 4H_2O\}_n$ (**2**) and $\{[Cu_2(L)_2(bpy)]\cdot 3H_2O\}_n$ (**3**), have been obtained under hydrothermal conditions. Compounds **1** and **2** show one-dimensional chain structures in which the [CuL] dimers and $[Cu(HL)_2]$ monomers are bridged by bpy, respectively. While, compound **3** has a layered structure in which the $[Cu_2(L)_2]$ tetramers are linked by bpy bridges. Weak antiferromagnetic interactions are found to be mediated between the copper centers in compounds **1** and **3**. Furthermore, we find the basic copper sources are crucial for the formation of the copper/phosphonate/bpy products.

References:

[1] Clearfield A, Demadis K D. *Metal Phosphonate Chemistry: From Synthesis to Applications*. London: The Royal Society of Chemistry, **2012**.

[2] Zhang Y, Clearfield A. *Inorg. Chem*., **1992**,**31**:2821-2826

[3] Zhang X L, Cheng K, Wang F, et al. *Dalton Trans*., **2014**,**43**: 285-289

[4] Drumel S, Janvier P, Bujoli-Doeuff M, et al. *Inorg. Chem*.,

1996,**35**:5786-5788

[5] Fu R B, Hu S M, Wu X T. *Cryst. Growth Des.*, **2015**,**15**: 3004-3014

[6] Bao S S, Li N Z, Taylor J M, et al. *Chem. Mater.*, **2015**,**27**: 8116-8125

[7] Ma Y S, Yin W Y, Cai W S, et al. *RSC Adv.*, **2013**,**3**:18430-18440

[8] Ma Y S, Zha L Q, Cai W S, et al. *Inorg. Chim. Acta*, **2013**, **406**:217-222

[9] Langley S, Helliwell M, Sessoli R, et al. *Inorg. Chem.*, **2008**, **47**:497-507

[10]Tang X Y, Zhong Q X, Hua J K, et al. *Inorg. Chim. Acta*, **2016**,**439**:77-81

[11]Ma Y S, Wang T W, Li Y Z, et al. *Inorg. Chim Acta*, **2007**, **360**:4117-4124

[12]McCabe D J, Rusell A A, Karthikeyan S, et al. *Inorg. Chem.*, **1987**,**26**:1230-1235

[13]Kahn O. *Molecular Magnetism*. New York: VCH Publishers Inc., **1993**.

[14]*CrystalClear*, Rigaku Corporation, Tokyo, Japan, **2005**.

[15]Sheldrick G M. *Acta Crystallogr. Sect. A*, **2008**,A64:112

[16]Ma Y S, Song Y, Du W X, et al. *Dalton Trans.*, **2006**:3228-3235